Motion of tracer particles in He II

D. R. Poole,[1] C. F. Barenghi,[1] Y. A. Sergeev,[2] and W. F. Vinen[3]
[1]*School of Mathematics, University of Newcastle, Newcastle upon Tyne, NE1 7RU, United Kingdom*
[2]*School of Mechanical and Systems Engineering, University of Newcastle, Newcastle upon Tyne, NE1 7RU, United Kingdom*
[3]*School of Physics and Astronomy, University of Birmingham, Birmingham B15 2TT, United Kingdom*
(Received 8 September 2004; revised manuscript received 10 December 2004; published 23 February 2005)

Recent experiments have shown that it is possible to implement particle image velocimetry (PIV) in liquid helium. However, to interpret the PIV data in the superfluid phase, it is necessary to understand how the particles are affected by the two components, the viscous normal fluid and the inviscid superfluid, as well as by the quantized vortex lines that may exist in the superfluid component. After setting up the governing equations of motion, we first solve them in some simple cases in order to gain physical insight, and then we formulate semiquantitative general arguments relating to turbulent flow, with the assumption initially that particle trapping by vortex lines does not occur. We find that a number of different but simple regimes can be identified if the particles are neutrally buoyant: in some regimes the particles trace the normal fluid, in others the superfluid, and in others the total mass current. A numerical analysis for a model two-dimensional flow reveals an instability that requires some modification of these conclusions. It is then shown that particle trapping on vortex lines can be important and can lead to serious modification of our conclusions. The results of our analysis are used to discuss what types of superfluid flow can usefully be studied by PIV, and to suggest the most appropriate size and mass of the tracer particles.

DOI: 10.1103/PhysRevB.71.064514 PACS number(s): 67.40.Vs, 47.80.+v, 47.27.−i

I. INTRODUCTION

The superfluid phase of liquid helium ^{4}He, or He II, to which we confine our attention, is a quantum fluid. According to the two-fluid model of Landau and Tisza,[1] it consists of the intimate mixture of two fluid components: the viscous normal fluid (of density ρ_n and velocity $\mathbf{v}_n$) and the inviscid superfluid (of density ρ_s and velocity $\mathbf{v}_s$). The total density of He II, $\rho=\rho_s+\rho_n$, is approximately temperature independent, but the relative proportions of normal fluid and superfluid, ρ_s/ρ and ρ_n/ρ, depend strongly on the temperature T. If T approaches the critical temperature, $T\rightarrow T_\lambda=2.17168$ K, the helium becomes entirely normal ($\rho_s/\rho\rightarrow 0$ and $\rho_n/\rho\rightarrow 1$); vice versa, in the limit of absolute zero, $T\rightarrow 0$ K, the helium becomes a pure superfluid ($\rho_s/\rho\rightarrow 1$ and $\rho_n/\rho\rightarrow 0$). At easily accessible temperatures below 1 K the normal fluid fraction can become negligible,[2] and the helium can then be considered for many purposes as a pure superfluid.

What makes He II particularly interesting is that rotational motion of the superfluid is constrained by quantum effects associated with discrete (quantized) vortex filaments. This quantized vorticity[3] has been the subject of great experimental and theoretical interest. Much current work is concerned with the observed similarity between quantum turbulence and classical turbulence,[4–8] something which is at first surprising, given the quantum restrictions and the two-fluid nature of the helium.

Given the hundreds of papers written on the fluid dynamics of He II, it is remarkable that there is so little direct experimental information about flow patterns. From the point of view of flow visualization, the comparison between quantum fluids and classical fluids is striking. In classical fluids a wide range of visualization techniques is available: ink, smoke, Kalliroscope flakes, hydrogen bubbles, Baker's pH technique, hot wire anemometry, laser Doppler anemometry, particle image velocimetry (PIV), and others. In He II there is as yet no direct way to determine flow patterns in either the normal fluid or the superfluid; the most widely used techniques (second sound and ion-trapping) probe only the vortex-line density averaged over a large volume. Measurements of temperature, pressure and chemical potential suffer the same problem of poor spatial resolution (but see Ref. 6). Turbulent fluctuations, especially on small scales, remain largely unexplored. There is no doubt that the study of superfluid flow, and especially superfluid turbulence, has been greatly impeded by the lack of suitable techniques of flow visualization.

Fortunately the need for flow-visualization techniques in liquid helium has recently been recognized, and appropriate techniques are now being developed. For example, Lucas and collaborators[9] have recently developed a cryogenic shadowgraph technique to reveal convection patterns. However, this technique depends on density variations caused by temperature fluctuations, so it cannot be immediately applied to the superfluid phase.

The subject of this paper is the PIV technique, which has been recently implemented with success in liquid helium by two experimental groups: that of Donnelly, Vinen, Niemela, and Sreenivasan[10] (until now in He I only) and that of VanSciver[11–13] (in He II). PIV is based on injecting many small tracer particles into the liquid. Two images are produced using short laser pulses of different colors (say, green and red) focused into a narrow sheet and separated in time by a few milliseconds. Software then analyzes the images and identifies green and red dots corresponding to the same particle at the two different times; in this way the observed distance between the corresponding dots yields the component of the local velocity in the plane of the light sheet. It must be stressed that, although PIV has been standard in

classical fluid dynamics for many years, its successful application to liquid He at temperatures near absolute zero was not simple and represents a useful achievement. The potential of PIV is great, particularly in the study of He II turbulence. However, there is a key question which must be answered before PIV data can be interpreted correctly: what do the tracer particles actually trace?

This question is far from trivial. The normal fluid is viscous so it exerts a drag force on the tracer particles; the superfluid is inviscid, so it causes no viscous drag. However, it is not correct to conclude that the particles trace only the normal fluid, because, in time-dependent flows (for example, turbulent flows), inertial effects can cause a tracer particle to respond also to superfluid motion. Furthermore, particles may become trapped on quantized vortex lines.

The plan of the paper is the following. In Sec. II we summarize the physical parameters of He II and of the tracer particles used in the experiments that are relevant to our discussion. In Sec. III we present the governing equations of motion of the particles and describe the approximations and the assumptions underlying them (mathematical details are contained in an Appendix). Section IV is concerned with the motion of particles in a fluid at rest under the influence of gravity. Section V is devoted to the case in which the normal fluid and the superfluid velocities have no spatial dependence but depend harmonically on time. We find that in some regimes the particles trace the normal fluid, in others the superfluid, in others the total mass current. In Sec. VI we use the resulting physical insight to suggest plausible semiquantitative results applicable to turbulent flows, but we ignore the possibility that the tracer particles might be trapped on quantized vortex lines. Section VII contains the results of numerical simulations of simple two-dimensional flows which apply to the case of vortex-coupled turbulence, in which the normal fluid and superfluid velocity fields are the same over a wide range of spatial scales due to the interaction through the quantized vortices; here we highlight a potential difficulty that, in some cases, the particle trajectory is unstable and spatial segregation may occur. Section VIII we examine the interaction between a tracer particle and a quantized vortex; we show that trapping is likely to occur in many practical cases, and we show that such trapping may lead to PIV observations that are difficult to interpret. Finally, Sec. IX summarizes our conclusions and points to further work.

As we have mentioned, a few experimental results on the application of PIV to superfluid ^{4}He have been published. Observations on thermal counterflow[12] are of particular interest and have shown that the tracer particles move with a velocity of approximately one half of the velocity of the normal fluid. We shall comment later on the significance of this result.

TABLE I. Parameters of He II.

T (K)	1.3	1.5	1.8	2.1
μ_n (μpoise)	15.3	13.5	13.0	18.0
ρ_s/ρ	0.955	0.899	0.687	0.259

II. FLUID AND PARTICLE PARAMETERS

The total density of liquid ^{4}He, ρ, is approximately independent of temperature and equal to 0.145 g cm^{-3}. Other relevant parameters are shown as functions of temperature in Table I: μ_n is the viscosity of the normal fluid; ρ_s/ρ is the superfluid fraction.

Specifications of the particles used so far by the different experimental groups are summarized in Table II. The particle radius is a; the effective (average) particle density is ρ_p.

In all cases the particle sizes are illustrative, in that each batch of particles has a certain distribution of size; the uniformity of the physical properties is an important factor which the experimentalists must take into account when deciding which kind of particle to use. In the experiments of Donnelly *et al.*[10] the heavier particles were allowed to fall towards the bottom of the apparatus, so that there was effective selection of particles that are, at least roughly, neutrally buoyant: $\rho_p \approx \rho$.

III. EQUATIONS OF MOTION

We consider the motion of a spherical particle of radius a and density ρ_p in superfluid ^{4}He, described by a two-fluid model. In the earlier parts of the paper (up to and including Sec. VII) we shall assume that the particles do not interact strongly with the quantized vortex lines in the superfluid component and are certainly not trapped by these lines. We make two further assumptions. The first assumption is that in the case of turbulent flow the presence of particles does not modify the turbulence (the assumed weak interaction between particles and vortex lines is a necessary but not sufficient condition for the validity of this assumption, which probably requires also that the particles be sufficiently small). The second assumption is that flow velocities vary by only a small fraction in distances of order a; this means that, for turbulent flow of the superfluid component, the particle

TABLE II. Specifications of the particles used in the experiments.

Authors	Material	a (μm)	ρ_p (g cm^{-3})
Van Sciver *et al.* (Refs. 11–13)	Solid neon particles	3–5	1.2
	Large hollow glass spheres	10–50	1.1
	Small hollow glass spheres	4–6	1.1
	Polymer microspheres	0.8	1.1
Donnelly *et al.* (Ref. 10)	Hollow glass spheres	1–5	roughly 0.145

must be small compared with the vortex line spacing, and, for turbulent flow of the normal fluid component, the particle must be small compared to the Kolmogorov length. Since it is relatively easier to achieve very intense turbulence in superfluid ^{4}He than in an ordinary fluid, the development of submicron size particles would be desirable.

It is clear that we need to generalize to our classical two-fluid model the equations of motion of a particle in a nonuniform flow in a classical fluid: an inviscid fluid[14] for the superfluid component, and a viscous fluid[15–17] for the normal fluid (detailed discussions of the two classical cases are contained in the Appendix). We make the assumption that the following equation represents a natural generalization:

$$\rho_p \vartheta \frac{d\mathbf{u}_p}{dt} = \mathbf{F}^{(\mathrm{g})} + \mathbf{F}_n^{(\mathrm{d})} + \mathbf{F}_n^{(\mathrm{i})} + \mathbf{F}_n^{(\mathrm{a})} + \mathbf{F}_n^{(\mathrm{B})} + \mathbf{F}_n^{(\mathrm{F})} + \mathbf{F}_n^{(\omega)} + \mathbf{F}_n^{(\mathrm{LM})} + \mathbf{F}_s^{(\mathrm{i})} + \mathbf{F}_s^{(\mathrm{a})} + \mathbf{F}_s^{(\omega)}, \tag{1}$$

where ϑ is the particle volume ($\vartheta = \frac{4}{3}\pi a^3$ for spherical particles), and $\mathbf{g}$ the acceleration due to gravity. In the right-hand side of Eq. (1), the subscripts "n" and "s" refer to the forces acting on the particle from the normal and superfluid components, respectively; the superscripts relate to contributions to the force on the particle as follows: (g) is the force due to gravity; (d) is the viscous drag force; (i) is the inertial force due to the carrier fluid acceleration (or the gradient of the pressure and shear stress); (a) is the added mass force; (B) is the Basset (history) force; (F) is the Faxén correction to the viscous drag; (ω) is the shear-induced lift force; and (LM) is the Magnus lift force. The gravity force is given by

$$\mathbf{F}^{(\mathrm{g})} = \vartheta(\rho_p - \rho)\mathbf{g}. \tag{2}$$

Hereafter we consider small particles such that the particle Reynolds number, relating to the normal fluid, is small; i.e., $\mathrm{Re}_p = 2\rho_n a|\mathbf{v}_n - \mathbf{u}_p|/\mu_n \ll 1$, so that the viscous drag force is linear in the relative velocity between the particle and the normal fluid. For a spherical particle we have

$$\mathbf{F}_n^{(\mathrm{d})} = 6\pi a \mu_n (\mathbf{v}_n - \mathbf{u}_p). \tag{3}$$

This expression for the drag force assumes that the roton mean free path $\lambda = 3\mu_n/(\rho_n v_G)$ is much smaller than the particle size a, where $v_G = \sqrt{2k_B T/(\pi m^*)}$ is the average thermal velocity of the rotons, k_B is Boltzmann's constant, $m^* = 0.16m$ is the roton effective mass, and $m = 6.65 \times 10^{-24}$ g is the mass of the helium atom. The condition $\lambda \ll a$ is satisfied for a typical particle size if $T > 1$ K (for example $\lambda \approx 10^{-6}$ cm at $T = 1.3$ K), but one must be aware of the existence of ballistic regimes at lower temperatures.

The inertial force due to an acceleration of the fluid has the same form for both inviscid and viscous components, i.e.,

$$\mathbf{F}_n^{(\mathrm{i})} = \rho_n \vartheta \frac{D\mathbf{v}_n}{Dt}, \quad \mathbf{F}_s^{(\mathrm{i})} = \rho_s \vartheta \frac{D\mathbf{v}_s}{Dt}. \tag{4}$$

Likewise, the form of the added mass force is identical for both fluids:

$$\mathbf{F}_n^{(\mathrm{a})} = C\rho_n \vartheta \left(\frac{D\mathbf{v}_n}{Dt} - \frac{d\mathbf{u}_p}{dt} \right), \quad \mathbf{F}_s^{(\mathrm{a})} = C\rho_s \vartheta \left(\frac{D\mathbf{v}_s}{Dt} - \frac{d\mathbf{u}_p}{dt} \right). \tag{5}$$

In Eqs. (4) and (5), the substantial derivatives of the normal and superfluid velocity, respectively, are defined as

$$\frac{D\mathbf{v}_n}{Dt} = \frac{\partial \mathbf{v}_n}{\partial t} + (\mathbf{v}_n \cdot \boldsymbol{\nabla})\mathbf{v}_n, \quad \frac{D\mathbf{v}_s}{Dt} = \frac{\partial \mathbf{v}_s}{\partial t} + (\mathbf{v}_s \cdot \boldsymbol{\nabla})\mathbf{v}_s. \tag{6}$$

The summary of the derivation of formulas (4) and (6) and a discussion of the assumptions behind this derivation, particularly the way in which viscous and inertial effects are combined, is given in the Appendix. The added mass coefficient C depends only on the particle geometry, and is the same for both inviscid and viscous fluids; see, e.g., Refs. 14, 15, and 18. For a spherical particle $C = \frac{1}{2}$. We note that the added mass effect is related to what physicists would usually describe as the effective mass of the particle when it moves in the fluid.

In the general case of nonuniform flow, the correct form of the forces $\mathbf{F}^{(\mathrm{i})}$ and $\mathbf{F}^{(\mathrm{a})}$ (containing the substantial derivative of the fluid velocity field, rather than the rate of change of the fluid velocity seen by the particle) was derived originally for the inviscid fluid (see, e.g., Ref. 14, although historically the first to derive the correct form of $\mathbf{F}^{(\mathrm{i})}$ and $\mathbf{F}^{(\mathrm{a})}$ was Taylor[19]). The equation of motion of the particle in the viscous flow was derived originally in Ref. 15 for the case of the time-dependent spatially uniform flow, for which the substantial derivatives in Eqs. (4) and (5) reduce to $d\mathbf{v}/dt$. The correct forms (4) and (5) for the forces $\mathbf{F}^{(\mathrm{i})}$ and $\mathbf{F}^{(\mathrm{a})}$ in the general case of spatially nonuniform viscous flow were proposed in Ref. 16 (see also Ref. 17).

In the approach typical of studies of particulate behavior in turbulent flows (see, e.g., Refs. 20 and 21) the Basset history force (A18) is usually neglected. Strictly speaking, this force is negligible only if the particle relaxation time τ, defined below in Eq. (11), is smaller than the time scale of the fluid motion.[22] For tracer particles in the turbulent flow this means that τ should be smaller than the turnover time τ_η of the smallest eddies. Suppose that the turbulence is characterized by a Kolmogorov energy spectrum, for which the fluid velocity on a scale b_η is of order $\epsilon^{1/3} b_\eta^{1/3}$, where ϵ is the rate of flow of energy per unit mass down the associated Richardson cascade (see Sec. VI A). The smallest eddies have a size equal to the Kolmogorov dissipation length, b_η, which is given by $b_\eta^4 = \epsilon^{-1}\nu^3$, where ν is the appropriate kinematic viscosity. It is then easily shown that the condition that the Basset history force be negligible is that the particle size, a, be small compared with $b_\eta(\rho_n/\rho)^{1/2}$; i.e., roughly that a must be small compared with the smallest length scale in the turbulence, which we have already assumed to be the case.

The Faxén correction to the viscous drag, $\mathbf{F}_n^{(\mathrm{F})}$ is of the order of $(a^2/L^2)\mathbf{F}_n^{(\mathrm{d})}$, where L is the length scale of the fluid motion, and it too can be neglected in the case where the particle size is smaller than the Kolmogorov dissipation length.

The transverse lift force $\mathbf{F}^{(\omega)}$ is quite different in each of the two fluids. In the superfluid component it is presumably of the form derived for a classical inviscid fluid:[14] $\mathbf{F}^{(\omega)} = C_L \rho \vartheta (\mathbf{v} - \mathbf{u}_p) \times \boldsymbol{\omega}$, where $\boldsymbol{\omega}$ is the vorticity, and C_L the lift coefficient, equal, for a sphere, to 0.5. Classically, it arises from the stretching of a uniform upstream vorticity around the particle as the fluid flows past it. In the normal component the transverse lift force has presumably the form of the shear-induced Saffman lift force, described in the Appendix.

Since we are assuming that the particles do not become trapped on vortex lines, they must remain in parts of the superfluid velocity field that are irrotational. Therefore the transverse lift force $\mathbf{F}_s^{(\omega)}$ must vanish. Behaviour can therefore be very different from that in a classical inviscid fluid.

Turning to the lift force from the normal fluid, we can compare its magnitude with that of the viscous drag on the particle. We note that the ratio of the shear-induced Saffman lift force $\mathbf{F}_n^{(\omega)}$ (see the Appendix) to the viscous drag can be estimated as

$$\frac{a \| \boldsymbol{\nabla} \mathbf{v}_n \|^{1/2}}{\nu^{1/2}} = \mathrm{Re}_p^{1/2} \left(\frac{a}{L} \right)^{1/2}, \tag{7}$$

where L is the length scale of the turbulence. Thus the Saffman lift force can be neglected if the particle Reynolds number is less than unity and if the particle size is less than the minimum value of L, which is the Kolmogorov dissipation length in the normal fluid (roughly equal in practice to the vortex-line spacing[7]).

A rotation of the particle combined with a finite relative velocity between the particle and the fluid will also induce the transverse Magnus force on the particle, $\mathbf{F}^{(\mathrm{LM})}$; see the Appendix. Although, in the case of small Reynolds numbers, this force is independent of the viscosity, the latter plays a crucial rôle in transferring a circulation from the particle to the fluid.[23] This justifies the form of the modeling equation of motion (1) where we assume that the Magnus lift force, given by Eq. (A22) with ρ replaced by ρ_n, acts on the particle from the normal fluid, but no such a force is exerted by the superfluid component whose viscosity is zero. In the absence of interparticle collisions the only mechanism inducing the particle rotation is the local shear in the ambient flow. In the considered case where the particle size is much smaller than the length scale of the flow, the vorticity can be considered as uniform (see subsection 2 of the Appendix). Since the vorticity $\boldsymbol{\omega}$ can be interpreted as twice the effective local angular velocity of the fluid, the magnitude of the particle angular velocity $|\boldsymbol{\Omega}|$ cannot be larger than $\frac{1}{2}|\boldsymbol{\omega}|$, so that the ratio of the Magnus lift force to the viscous drag cannot exceed

$$\frac{\pi a^3 \rho_n |\boldsymbol{\omega}| |\mathbf{v}_n - \mathbf{u}_p|}{6 \pi a \mu_n |\mathbf{v}_n - \mathbf{u}_p|} \sim \frac{\rho_n a |\mathbf{v}_n - \mathbf{u}_p|}{\mu_n} \frac{a \| \boldsymbol{\nabla} \mathbf{v}_n \|}{|\mathbf{v}_n - \mathbf{u}_p|} \sim \varepsilon \, \mathrm{Re}_p, \tag{8}$$

where ε is the small parameter introduced by Eq. (A1). From Eqs. (7) and (8) it follows that, in the case where the particle size is less than the smallest length scale of the flow, the Magnus force is much smaller than the Saffman lift force (indeed, $|\mathbf{F}_n^{(\mathrm{LM})}| / |\mathbf{F}_n^{(\omega)}| \lesssim \varepsilon^{1/2} \, \mathrm{Re}_p^{1/2}$).

We conclude then that all the forces $\mathbf{F}_n^{(B)}$, $\mathbf{F}_n^{(F)}$, $\mathbf{F}_n^{(\omega)}$, $\mathbf{F}_s^{(\omega)}$, and $\mathbf{F}_n^{(\mathrm{LM})}$ can probably be neglected if the particle size is less than the smallest scale of the turbulence and if there is no trapping of particles on vortex lines, assumptions that we made at the start of the discussion in this section.

With the above assumptions we arrive at the following modeling equation of the particle motion:

$$\begin{aligned} \rho_p \vartheta \frac{d\mathbf{u}_p}{dt} = {} & 6 \pi a \mu_n (\mathbf{v}_n - \mathbf{u}_p) + \vartheta (\rho_p - \rho) \mathbf{g} + \rho_n \vartheta \frac{D\mathbf{v}_n}{Dt} \\ & + C \rho_n \vartheta \left(\frac{D\mathbf{v}_n}{Dt} - \frac{d\mathbf{u}_p}{dt} \right) + \rho_s \vartheta \frac{D\mathbf{v}_s}{Dt} \\ & + C \rho_s \vartheta \left(\frac{D\mathbf{v}_s}{Dt} - \frac{d\mathbf{u}_p}{dt} \right). \end{aligned} \tag{9}$$

In the absence of gravity, after setting $C = 1/2$, it is convenient to rewrite this equation as

$$\frac{d\mathbf{u}_p}{dt} = \frac{1}{\tau} (\mathbf{v}_n - \mathbf{u}_p) + \frac{3}{2\rho_o} \left(\rho_n \frac{D\mathbf{v}_n}{Dt} + \rho_s \frac{D\mathbf{v}_s}{Dt} \right), \tag{10}$$

where ρ_o and the viscous relaxation time, τ are given by

$$\rho_o = \rho_p + \frac{\rho}{2}, \quad \tau = \frac{2a^2 \rho_o}{9 \mu_n}. \tag{11}$$

In the case of neutrally buoyant particles ($\rho_p = \rho$) the parameters ρ_o and τ reduce to

$$\rho_o = \frac{3}{2} \rho, \quad \tau = \frac{\rho a^2}{3 \mu_n}. \tag{12}$$

IV. SEDIMENTATION

If the normal fluid and the superfluid are both stationary ($\mathbf{v}_n = \mathbf{v}_s = 0$), then, in the presence of gravity and starting from the initial condition $\mathbf{u}_p = 0$, the equation of motion is $\rho_p \vartheta d\mathbf{u}_p / dt = -6 \pi a \mu_n \mathbf{u}_p + \vartheta (\rho_p - \rho) \mathbf{g}$. After an initial transient, the particle achieves the terminal speed

$$u_\infty = \frac{2}{9} \frac{a^2 g (\rho_p - \rho)}{\mu_n}, \tag{13}$$

with the time scale (known as the particle response time)

$$\tau_\infty = \frac{2}{9} \frac{a^2 \rho_p}{\mu_n}. \tag{14}$$

These formulas can be used to determine the particle size a[11], provided, of course, that the particles are not neutrally buoyant. For the polymer microspheres used by Van Sciver and collaborators[12] we have $a \approx 8 \times 10^{-5}$ cm and $\rho_p \approx 1.1$ g cm^{-3}; thus, at $T = 1.5$ K, the terminal speed is $u_\infty \approx 0.10$ cm/s, and the particles response time is $\tau_\infty \approx 0.12 \times 10^{-3}$ s.

In the following sections we consider sufficiently small particles such that their terminal sedimentation velocity (14) is small compared with characteristic velocities of the flow; then we can neglect gravity in the particle equation of motion.

V. TIME-DEPENDENT FLOWS WITH NO SPATIAL DEPENDENCE

We assume that the velocities of the normal fluid and the superfluid have no spatial dependence but have harmonic time dependence $\mathbf{v}_n = \mathbf{V}_n \exp(i\omega t)$ and $\mathbf{v}_s = \mathbf{V}_s \exp(i\omega t)$, where ω is the angular frequency. (Our neglect of the trapping of particles by vortex lines is then irrelevant). Then in Eq. (10) $D\mathbf{v}_n/Dt = d\mathbf{v}_n/dt$ and $D\mathbf{v}_s/Dt = d\mathbf{v}_s/dt$, where d/dt is an ordinary derivative, so that the solution of Eq. (10) is

$$\mathbf{u}_p = \mathbf{U}_p^{(0)} \exp\left(-\frac{t}{\tau}\right) + \mathbf{U}_p \exp(i\omega t), \tag{15}$$

where the transient term $\mathbf{U}_p^{(0)} \exp(-t/\tau)$ allows for an arbitrary initial particle velocity $\mathbf{u}_p(0)$ at $t=0$, and the term

$$\mathbf{U}_p = \frac{1}{(1+i\omega\tau)}\left[\left(1+\frac{3i\omega\tau\rho_n}{2\rho_o}\right)\mathbf{V}_n + \left(\frac{3i\omega\tau\rho_s}{2\rho_o}\right)\mathbf{V}_s\right] \tag{16}$$

is the steady-state response of the particle.

Equation (16) has two interesting limits. If $\omega\tau \gg 1$, then the steady-state response is given by $\mathbf{U}_p = \frac{3}{2}\rho^{-1}(\rho_n\mathbf{V}_n + \rho_s\mathbf{V}_s)$, while if $\omega\tau \ll 1$ then it is given by $\mathbf{U}_p = \mathbf{V}_n$, that is to say the particles track the normal fluid.

The case of particles that are neutrally buoyant is particularly simple. In the limit $\omega\tau \gg 1$ we have $\mathbf{U}_p = \rho^{-1}(\rho_n\mathbf{V}_n + \rho_s\mathbf{V}_s)$, which means that the particles move with a velocity corresponding to the total current density ($\mathbf{j} = \rho_n\mathbf{v}_n + \rho_s\mathbf{v}_s$), which is equal to zero in, for example, a second sound wave, and is equal to simply $\mathbf{v}_s$ at very low temperatures. In the limit $\omega\tau \ll 1$ we have again $\mathbf{U}_p = \mathbf{V}_n$, so the particles move with the normal component. These results show that, from a practical point of view, the use of neutrally buoyant particles is obviously convenient, since they do not tend to be lost by sedimentation and the particle velocity is rather simply related to the velocities of the two fluids.

We note that the transient term in Eq. (15) must die out at times large compared to the relaxation time τ (it does not vanish therefore at $T=0$). It is interesting to note the behavior of the particle velocity in response to a step-function change $\Delta\mathbf{v}_s$ in $\mathbf{v}_s$ at $t=0$. If $\mathbf{v}_n = 0$, the particle velocity is given by

$$\frac{d\mathbf{u}_p}{dt} = -\frac{\mathbf{u}_p}{\tau} + \frac{\rho_s}{\rho}\frac{d\mathbf{v}_s}{dt}, \tag{17}$$

so that the particle velocity jumps from zero to $(\rho_s/\rho)\Delta\mathbf{v}_s$ at $t=0$ and then decays with time constant τ.

In cases when the superfluid and normal fluid velocities are the same, $\mathbf{v}_n = \mathbf{v}_s = \mathbf{v}$ (see Sec. VII), the particle velocity is given by

$$\frac{d}{dt}(\mathbf{u}_p - \mathbf{v}) = -\frac{\mathbf{u}_p - \mathbf{v}}{\tau}, \tag{18}$$

from which we see that, after an initial transient, the particle velocity ought faithfully to follow $\mathbf{v}$ for all time-dependences of $\mathbf{v}$. Physically there is a simple reason for this behavior. After the initial transient, the force on the particle (arising from pressure gradients in the fluid) is exactly the same as the force on the volume of fluid that replaces the particle. Therefore the particle must move in the same way as this volume of fluid. Note however that this conclusion, obtained here for spatially-independent flows, may be affected by issues of stability in the case of spatially-dependent flows (as discussed in Sec. VII).

VI. TURBULENT FLOW

More generally, $\mathbf{v}_n$ and $\mathbf{v}_s$ depend both on time and space. With the assumption that the particles are neutrally buoyant ($\rho_p = \rho$), Eq. (10) takes the form

$$\frac{d\mathbf{u}_p}{dt} = \frac{1}{\tau}(\mathbf{v}_n - \mathbf{u}_p) + \frac{\rho_n}{\rho}\left[\frac{\partial\mathbf{v}_n}{\partial t} + (\mathbf{v}_n\cdot\boldsymbol{\nabla})\mathbf{v}_n\right] + \frac{\rho_s}{\rho}\left[\frac{\partial\mathbf{v}_s}{\partial t} + (\mathbf{v}_s\cdot\boldsymbol{\nabla})\mathbf{v}_s\right]. \tag{19}$$

To understand what is predicted by Eq. (19) it is instructive to consider for a moment the simpler equation

$$\frac{d\mathbf{u}_p}{dt} = \left[\frac{\partial\mathbf{v}}{\partial t} + (\mathbf{v}\cdot\boldsymbol{\nabla})\mathbf{v}\right] \tag{20}$$

describing the motion of a neutrally buoyant particle in a single incompressible fluid in the absence of viscosity and in regions where the flow is irrotational. The motion of this fluid is described by the Euler equation, which is

$$\frac{\partial\mathbf{v}}{\partial t} + (\mathbf{v}\cdot\boldsymbol{\nabla})\mathbf{v} = -\frac{1}{\rho}\boldsymbol{\nabla}p, \tag{21}$$

where p is the pressure. Equation (20) thus becomes

$$\frac{d\mathbf{u}_p}{dt} = -\frac{1}{\rho}\boldsymbol{\nabla}p. \tag{22}$$

The right-hand side is equal to the force per unit mass acting on an element of the fluid in the absence of viscosity, and is also equal to the force on the particle that replaces, and moves with, this volume in the fluid. This force causes the particle to accelerate at the same rate as does the displaced element of fluid. Therefore, apart from a possible transient, Eq. (20) predicts that the particle will move with the fluid, even in the absence, as here, of viscosity. Of course in a sense this conclusion must obviously be true, and it confirms that we are using the correct equations of motion for the particle. However, as we shall see later, the conclusion is not quite correct. Although it is true that this predicted motion of the particle is a solution of Eq. (29), it turns out, as we shall see later, that the motion is not completely stable, although the instability may become apparent only after a significant time has elapsed.

Returning to Eq. (19), we make use of the two-fluid equations, which are[3]

$$\rho_s\frac{D\mathbf{v}_s}{Dt} = -\frac{\rho_s}{\rho}\boldsymbol{\nabla}p + \rho_s S\boldsymbol{\nabla}T, \quad \rho_n\frac{D\mathbf{v}_n}{Dt} = -\frac{\rho_n}{\rho}\boldsymbol{\nabla}p - \rho_s S\boldsymbol{\nabla}T + \mu_n\boldsymbol{\nabla}^2\mathbf{v}_n, \tag{23}$$

where S is the specific entropy. We have omitted any force of mutual friction. This is because such a force arises from the

interaction of the vortex cores with the normal fluid, so that it is unimportant in regions of the flow remote from the vortex cores, where, according to our assumptions, the particle is situated.

Substituting from Eqs. (23) into Eq. (19), we see that the temperature gradients cancel out, leaving

$$\frac{d\mathbf{u}_p}{dt} = \frac{1}{\tau}(\mathbf{v}_n - \mathbf{u}_p) - \frac{1}{\rho}\boldsymbol{\nabla} p + \frac{\mu_n}{\rho}\boldsymbol{\nabla}^2\mathbf{v}_n. \tag{24}$$

Neglecting the viscosity of the normal fluid, Eq. (24) reduces to Eq. (22), which says that the force on the particle is due to the pressure gradient alone. But the pressure gradient, if it were to act alone on the fluid, would cause an acceleration of the whole fluid, i.e., a change in the total current density $\mathbf{j} = \rho_n\mathbf{v}_n + \rho_s\mathbf{v}_s$. We conclude that, apart from possible transients, and with neglect of the viscosity of the normal fluid, the particle will move with velocity $\mathbf{j}/\rho$, as in the situation described in a previous section.

A. Homogeneous turbulence without steady mean counterflow

We now take into account the effects of viscosity, returning to Eq. (19), and apply our consideration to fully developed homogeneous turbulence. We still neglect the possibility that particles may be trapped on vortex lines. We also assume for the present that the turbulence is not accompanied by any steady average flow or counterflow, and we use a frame of reference in which the time-averaged fluid velocities vanish. We imagine that turbulence in each fluid involves a range of eddy sizes, with a Richardson cascade, and with viscouslike dissipation on a small scale. We focus on a length scale b within the inertial range $b_\eta \ll b \ll b_0$ where b_0 is the (large) scale at which energy is fed into the cascade, and b_η is the (small) scale at which the energy is destroyed (the Kolmogorov length). At the scale b the velocities are of the order $v_s(b)$ and $v_n(b)$. The nonlinear terms in Eq. (19) are those which lead in the Navier-Stokes equation to the transfer of energy to different length scales, and this transfer is most effective between neighboring scales. The transfer process gives rise to a finite lifetime for eddies of size b, equal in order of magnitude to the "turnover time" $\tau_s(b) \approx b/v_s(b)$ and $\tau_n(b) \approx b/v_n(b)$. It follows that the motion on the length scale b is likely to make contributions to the two terms in square brackets in Eq. (19) of the order $v_s(b)/\tau_s \approx v_s^2(b)/b$ and $v_n(b)/\tau_n \approx v_n^2(b)/b$.

When comparing these two terms with the first term of the equation, $(\mathbf{v}_n - \mathbf{u}_p)/\tau$, we distinguish between the following two limits. If the turnover times τ_s and τ_n are significantly less than the relaxation time τ, the term $(\mathbf{v}_n - \mathbf{u}_p)/\tau$ can be neglected and the particle will move with the velocity $\mathbf{j}/\rho$ induced by the two terms within the square bracket in Eq. (19). In the opposite limit, if τ_s and τ_n are significantly larger than τ, the particle will move with the normal fluid (besides issues of stability of the trajectory).

At very low temperatures τ becomes very large (small viscous drag) and the normal fluid density becomes very small. The particle will then follow the turbulence in the superfluid component.

It is instructive to estimate the relative magnitudes of the viscous relaxation time, τ, and the turnover times, τ_s and τ_n, at higher temperatures (above 1 K), where the drag on a particle is described by the Stokes law [Eq. (3)]. Consider, for example, the case of grid turbulence in superfluid ^{4}He[7]. In this case it is believed that each fluid has essentially the same turbulent velocity field, characterized by a Richardson cascade, with a Kolmogorov spectrum, on length scales large enough for dissipative processes to be unimportant. Such *vortex-coupled turbulence* can arise because the turbulence in each fluid has a natural tendency to have the same Kolmogorov form, the two velocity fields being accurately locked together by mutual friction. For a Kolmogorov spectrum the turbulent velocity associated with eddies on a scale b is given by $v^2(b) \approx \epsilon^{2/3}b^{2/3}$. The turnover time, $\tau(b)$, associated with these eddies is then $b/v(b)$. For a classical fluid with kinematic viscosity ν the Richardson cascade is terminated by viscous dissipation at the Kolmogorov dissipation length scale given by $b_\eta^4 \approx \nu^3/\epsilon$. In the case of the vortex-coupled turbulence there is dissipation, due to a combination of normal fluid viscosity and mutual friction, on a length scale of the order of vortex-line spacing, so that this spacing acts as an effective value of b_η. At the same time the effective kinematic viscosity is of order μ_n/ρ, where ρ is the total density of the helium.[7] Thus we find that

$$\frac{\tau(b)}{\tau} \approx 3\left(\frac{b}{b_\eta}\right)^{2/3}\left(\frac{b_\eta}{a}\right)^2. \tag{25}$$

Since we are assuming that the particle size is much less than the minimum length scale in the turbulence, the ratio $(b_\eta/a)^2$ must be large compared with unity. Furthermore, the ratio (b/b_η) must be equal to or larger than unity, since there is no turbulence on a length scale less than b_η. It follows that in all circumstances $\tau(b) \gg \tau$, so that, according to our assumptions, the particle must follow the normal fluid.

B. Turbulence with steady uniform mean counterflow

We now extend this treatment to the special case when the two fluids are in steady and uniform average relative motion, each fluid itself moving with a spatially uniform velocity and having a spatially homogeneous turbulent velocity field. Such a flow is a model for counterflow turbulence in superfluid ^{4}He. We start in an arbitrary inertial frame of reference, in which the mean values of the particle, normal fluid and superfluid velocity, respectively, are $\langle\mathbf{u}_p\rangle$, $\langle\mathbf{v}_n\rangle$, and $\langle\mathbf{v}_s\rangle$. Equation (19) then takes the form

$$\begin{aligned}\frac{d\mathbf{u}_p'}{dt} + \frac{d\langle\mathbf{u}_p\rangle}{dt} = &-\frac{\mathbf{u}_p' - \mathbf{v}_n'}{\tau} - \frac{\langle\mathbf{u}_p\rangle - \langle\mathbf{v}_n\rangle}{\tau} \\ &+ \frac{\rho_n}{\rho}\left[\frac{\partial\mathbf{v}_n'}{\partial t} + (\mathbf{v}_n'\cdot\boldsymbol{\nabla})\mathbf{v}_n' + (\langle\mathbf{v}_n\rangle\cdot\boldsymbol{\nabla})\mathbf{v}_n'\right] \\ &+ \frac{\rho_s}{\rho}\left[\frac{\partial\mathbf{v}_s'}{\partial t} + (\mathbf{v}_s'\cdot\boldsymbol{\nabla})\mathbf{v}_s' + (\langle\mathbf{v}_s\rangle\cdot\boldsymbol{\nabla})\mathbf{v}_s'\right],\end{aligned} \tag{26}$$

where primes denote fluctuations of the velocities above the

mean. Averaging over space, and using the assumption that the turbulence in each fluid is homogeneous, we find that

$$\frac{d\langle \mathbf{u}_p \rangle}{dt} = -\frac{\langle \mathbf{u}_p \rangle - \langle \mathbf{v}_n \rangle}{\tau}, \tag{27}$$

so that after a transient the average velocity of the particle is equal to the average velocity of the normal fluid. Subtracting Eq. (27) from Eq. (26) we obtain the equation describing the fluctuations in the particle velocity:

$$\frac{d\mathbf{u}_p'}{dt} = -\frac{\mathbf{u}_p' - \mathbf{v}_n'}{\tau} + \frac{\rho_n}{\rho}\left[\frac{\partial \mathbf{v}_n'}{\partial t} + [(\langle \mathbf{v}_n \rangle + \mathbf{v}_n') \cdot \boldsymbol{\nabla}]\mathbf{v}_n'\right] + \frac{\rho_s}{\rho}\left[\frac{\partial \mathbf{v}_s'}{\partial t} + [(\langle \mathbf{v}_s \rangle + \mathbf{v}_s') \cdot \boldsymbol{\nabla}]\mathbf{v}_s'\right]. \tag{28}$$

We note that both the viscous term and each term in square brackets are invariant to an inertial transformation of coordinates, although the individual terms within each square bracket are not invariant. It follows that we can evaluate each term separately in any convenient frame. The first term in square brackets can be considered conveniently in a frame moving with the mean velocity $\langle \mathbf{v}_n \rangle$ of the normal fluid, while the second term in square brackets in a frame moving with the mean velocity $\langle \mathbf{v}_s \rangle$ of the superfluid. It follows that the fluctuations in the particle velocity are independent of the mean steady counterflow. Thus, generally, the particle follows the average motion of the normal fluid, after the relaxation time τ allows $\langle \mathbf{u}_p \rangle$ to become equal to $\langle \mathbf{v}_n \rangle$, but otherwise it senses only the turbulent fluctuations in the velocity fields of the two fluid in the same way as it would if the mean flows were absent.

Our conclusion that the average particle velocity is equal to the average velocity of the normal fluid is not in agreement with recent experimental results.[12] We return to this matter later.

VII. VORTEX-COUPLED TURBULENCE

Recent experiments[4–6] and theoretical work[7,8] suggest that, if He II is made turbulent by agitating it with a towed grid or rotating propellers, then a rather simple form of turbulence is produced. Both fluids become turbulent, the turbulence in both cases being essentially classical on length scales greater than those on which dissipation occurs, which turns out to be comparable with the average vortex line spacing $\ell \approx L_0^{-1/2}$; furthermore, the mutual friction between the two fluids, arising from the presence of vortex lines in the superfluid component, ensures that not only is the turbulence classical in form but also that the two velocity fields are essentially identical: $\mathbf{v}_n = \mathbf{v}_s = \mathbf{v}$, where $\mathbf{v}$ represents the vortex-coupled turbulent velocity. This idea has already been mentioned in connection with grid turbulence in Sec. VI A. It can be argued, therefore, that, on scales larger than the vortex-line spacing the governing equation of motion (10) reduces to

$$\frac{d\mathbf{u}_p}{dt} = \frac{\mathbf{v} - \mathbf{u}_p}{\tau} + \gamma \frac{D\mathbf{v}}{Dt}, \tag{29}$$

where $D\mathbf{v}/Dt = \partial \mathbf{v}/\partial t + (\mathbf{v} \cdot \boldsymbol{\nabla})\mathbf{v}$ and $\gamma = 3\rho/(2\rho_o)$. For neutrally buoyant particles $\gamma = 1$.

We emphasize that the two velocity fields coincide only on length scales significantly larger than the minimum length scale provided by the vortex line spacing,[7] so that our representation will not be good for vortex-coupled turbulence on the smallest length scales. However, as we shall explain, our principal motivation in this section is to explore an instability in the particle trajectories to which we have already referred several times, and our approach, which is really to treat the helium as a single viscous fluid, is adequate for this purpose.

Note that, for $\gamma = 1$, $\mathbf{u}_p(t) \equiv \mathbf{v}(\mathbf{r}(t), t)$ is a formal solution of Eq. (29), where $\mathbf{r}(t)$ is a trajectory of a fluid particle (passive scalar), because the Lagrangian time derivative $d\mathbf{u}_p/dt$ seen by the particle coincides with the substantial derivative D/Dt of the fluid velocity. It would therefore seem natural to conclude that neutrally buoyant particles should follow the fluid exactly, and that almost buoyant particles should trace the fluid almost exactly.

However, it has been known for some time that particles with density larger than that of the fluid are expelled from regions of high vorticity, and that they cluster, eventually, in the regions of high rate of strain and low vorticity. In contrast, particles with density lower than that of the fluid are drawn towards regions of high vorticity (see, e.g., Refs. 24 and 25 and references therein). Moreover, recent work[26] has indicated that even the motion of a neutrally buoyant particle is unstable, and that particle trajectories differ from those of an ideal passive scalar.

Note that the only situation where the formal solution $\mathbf{u}_p(t) \equiv \mathbf{v}(\mathbf{r}(t), t)$ is stable is the case of very low temperatures. In this case the normal fluid is absent, $\mathbf{v} \equiv \mathbf{v}_s$, and Eq. (29) becomes, for neutrally buoyant particles ($\gamma = 1$), a kinematic equation for fluid points. Such an equation obviously has a neutrally stable solution $\mathbf{u}_p \equiv \mathbf{v}_s$. (However, even in this case there are potential sources for instability, such as the finite size of the particle, and the fact that the particle density is unlikely to be precisely equal to the fluid density).

Clearly the issue of the stability of particle trajectories must be taken into account when using the PIV method to study turbulence in He II, including the special case of vortex-coupled turbulence. Real turbulent flows are hard to treat, so it is instructive to study the motion of particles in simpler, two-dimensional, flows in order to gain physical insight into what happens in real turbulent flows. The governing equations of motion must be solved numerically, but the computational difficulty is much less than in the case of three-dimensional flows. To model the turbulent velocity field $\mathbf{v}$ we use the Arnold-Beltrami-Childress (ABC) flow[27–29] and set $\mathbf{v} = \mathbf{v}^{\mathrm{ABC}} = (v_x^{\mathrm{ABC}}, v_y^{\mathrm{ABC}}, v_z^{\mathrm{ABC}})$, where the components of $\mathbf{v}^{\mathrm{ABC}}$ at the point $\mathbf{r} = (x, y, z)$ are

$$v_x^{\mathrm{ABC}} = A \sin(2\pi z) + C \cos(2\pi y),$$

$$v_y^{\mathrm{ABC}} = B \sin(2\pi x) + A \cos(2\pi z),$$

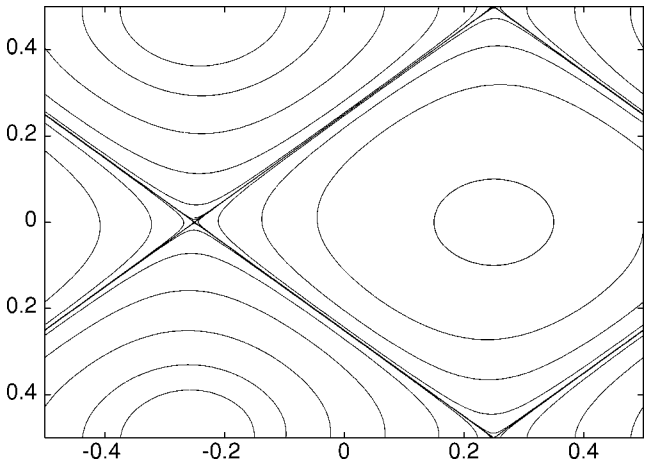

FIG. 1. Plot of the path lines of a two-dimensional ABC flow ($A=B$ and $C=0$) in the (x,z) plane.

$$v_z^{\mathrm{ABC}} = C\sin(2\pi y) + B\cos(2\pi x), \tag{30}$$

and A, B, and C are given parameters. The use of an ABC flow is motivated by simplicity and computational convenience. ABC flows are solutions of the steady Euler equation and of the time dependent, forced Navier-Stokes equation. Despite the simple functional form, they represent a relatively complex spatial structure consisting of six vortex tubes of positive and negative circulation aligned parallel to the Cartesian axes within the unit box $(-1/2 \leqslant x \leqslant 1/2,\ -1/2 \leqslant y \leqslant 1/2,\ -1/2 \leqslant z \leqslant 1/2)$. ABC flows thus provide idealized models of turbulent vortex structures, and for this purpose they have been used in applications ranging from astrophysical fluid dynamics[30] to superfluidity.[31] For the sake of simplicity we choose $A=B$ and $C=0$, a condition which guarantees that the flow is two-dimensional; this restriction does not affect our results and serves to simplify their graphical presentation.

To visualize the ABC flow we follow the motion of a number of fluid particles (distinct from tracer particles) by integrating the equation $d\mathbf{r}_p/dt = \mathbf{v}^{\mathrm{ABC}}$ using a semi-implicit Crank-Nicholson method.[32] The resulting path lines are shown in Fig. 1.

We now proceed to simulate numerically the motion of the tracer particles using the ABC flow model. Our numerical simulations start at time $t=0$ by placing an ensemble of N particles (typically $N=1000$) at random positions in the computational box. For simplicity we assume that all particles have the same size and density. The initial velocity of a particle at position $\mathbf{r}=\mathbf{r}_p$ is equal to the fluid velocity at that position. The particle position $\mathbf{r}_p$ and velocity $\mathbf{u}_p$ are then integrated in time by solving Eq. (29) for $\mathbf{u}_p$ and the equation $d\mathbf{r}_p/dt = \mathbf{u}_p$ for $\mathbf{r}_p$; periodic boundary conditions are used. Since the lifetime of eddies in a turbulent flow is typically of the order of the turnover time, we stop the calculation at the final time $t = 3\tau_{\mathrm{ABC}} = 2\pi/|\boldsymbol{\omega}^{\mathrm{ABC}}|$ where $\boldsymbol{\omega}^{\mathrm{ABC}} = \boldsymbol{\nabla}\times\mathbf{v}^{\mathrm{ABC}} = 2\pi\mathbf{v}^{\mathrm{ABC}}$, for which $\tau_{\mathrm{ABC}} = (A^2+B^2+C^2)^{-1/2}$.

First we consider the case of particles that are not neutrally buoyant. We choose $\rho_p = 1.1$ g/cm^3 and a range of values of radius centred around $a = 8.5\times10^{-5}$ cm. We assume

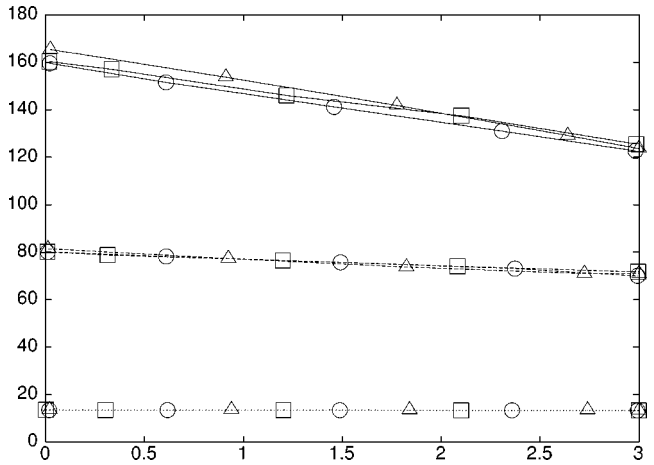

FIG. 2. Plot of $\langle|\mathbf{u}_p|\rangle$ as a function of t/τ_{ABC}. Solid lines correspond to $A=B=120$ cm/s, dashed lines to $A=B=60$ cm/s, and dotted lines to $A=B=10$ cm/s. The symbols correspond to different values of the radius of the particles: Squares: $a=8.075\times10^{-5}$ cm; circles: $a=8.5\times10^{-5}$ cm; triangles: $a=8.925\times10^{-5}$ cm. In all runs $C=0$, $T=2$ K, and $\rho_p=1.1$ g/cm^3.

that the temperature is $T=2$ K, for which $\rho_n = 0.08055$ g cm^{-3} and $\rho_s = 0.06507$ g cm^{-3}. The choice of velocity range is motivated by the orders of magnitude achieved in the Oregon towed-grid experiments,[5] and we take three values of A: 120 cm/s, 60 cm/s, and 10 cm/s (with $B=A$ and $C=0$). To measure the ability of the particles to track the fluid, we calculate the ensemble-averaged velocity of the particles, $\langle|\mathbf{u}_p|\rangle$, and the ensemble-averaged velocity of the fluid evaluated at the position of each particle, $\langle|\mathbf{v}^{\mathrm{ABC}}|\rangle$. Figure 2 shows $\langle|\mathbf{u}_p|\rangle$ plotted versus t/τ_{ABC}, and Fig. 3 shows the ensemble-averaged relative difference between the velocity of the particles and the velocity of the fluid at the position of the particles (note the logarithmic scale). It is apparent that, after an initial transient, the particles trace the fluid rather well, particularly the smaller particles at the smaller velocities.

Note in Fig. 2 that, at relatively large flow velocity, $\langle|\mathbf{u}_p|\rangle$ (and also $\langle|\mathbf{v}^{\mathrm{ABC}}|\rangle$) decreases with time. This is a conse-

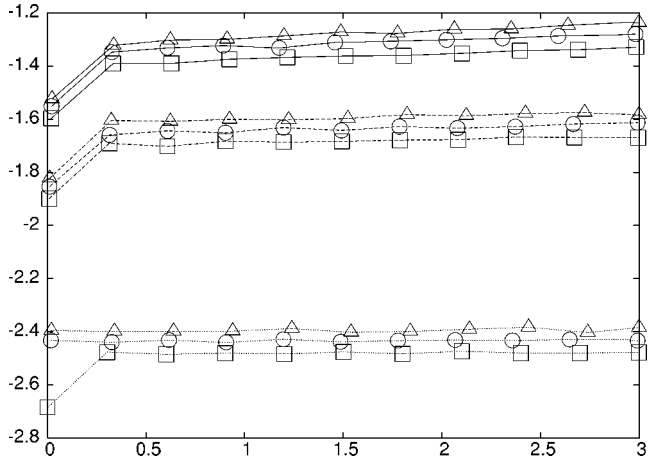

FIG. 3. Plot of $\log_{10}(\langle|\mathbf{u}_{\mathrm{p}}-\mathbf{v}^{\mathrm{ABC}}|/|\mathbf{v}^{\mathrm{ABC}}|\rangle)$ as a function of t/τ_{ABC}. Lines and symbols correspond to those of Fig. 2. In all runs $C=0$, $T=2$ K, and $\rho_p=1.1$ g/cm^3.

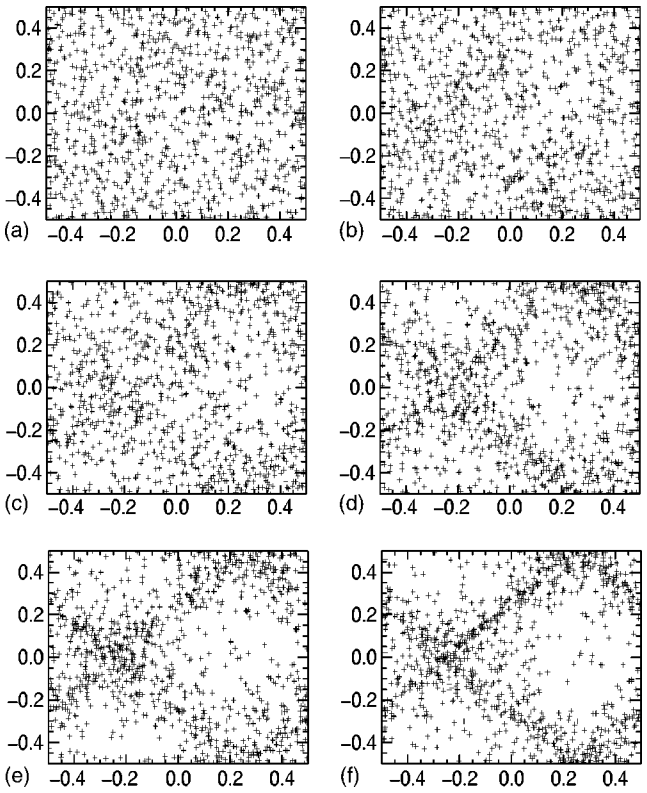

FIG. 4. Position of tracer particles in the (x,z) plane ($a=8.075\times10^{-5}$ cm and $\rho_p=1.1$ g cm^{-3}) at different times. Calculation performed at $T=2$ K and ABC flow intensity $A=B=120$ cm/s, $C=0$, for which $\tau_{\mathrm{ABC}}=5.89\times10^{-3}$ s: (a) $t=0.0$ s, (b) $t=3.53\times10^{-3}$ s, (c) $t=7.06\times10^{-3}$ s, (d) $t=1.06\times10^{-2}$ s, (e) $t=1.41\times10^{-2}$ s, and (f) $t=1.76\times10^{-2}$ s$=3\tau_{\mathrm{ABC}}$.

quence of the spatial segregation resulting from the instability of particle trajectories mentioned above. The effect is made clear if we consider the actual positions of the particles in the flow, as we see in Fig. 4. Initially the particles are randomly scattered throughout the computational box. As time progresses, the particles are expelled from the regions where the vorticity is large and segregate into the regions where the rate of strain is large; this is evident if we compare the final position of the particles in Fig. 4 against the ABC path lines of Fig. 1. We conclude that the apparently good result shown in Fig. 3 may hide a difficulty: the particles seem to trace the flow fairly well, but, particularly for large velocities, the trajectories are unstable, and the particles segregate spatially, moving from the regions of large vorticity to the regions of large strain rate. Since $C=0$, it should be expected that the initial random scatter of particles be preserved in (x,y) and (y,z) planes, and this is indeed the case, as we have verified numerically.

At smaller flow velocities (say $A=B=10$ cm/s, $C=0$), the ensemble-averaged velocity $\langle|\mathbf{u}_p|\rangle$ does not decrease with time (Fig. 2), and indeed if we look at the distribution of particles in the (x,z) plane over the same time scale τ/τ_{ABC} we see no sign of segregation.

To obtain a more quantitative understanding of how the expulsion from the eddies depends on the particle size and the intensity of the turbulent flow we define two regions in

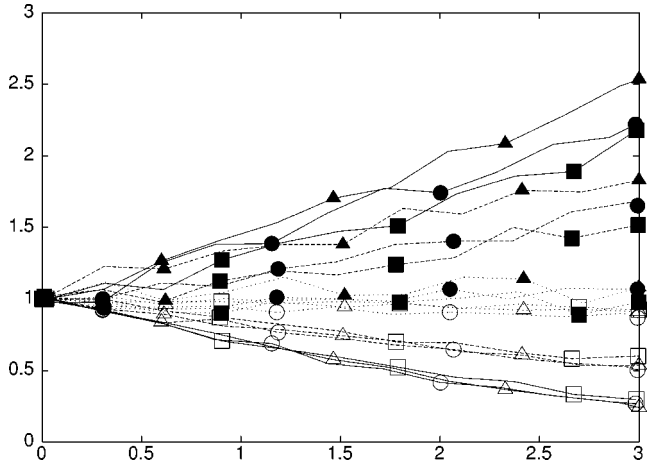

FIG. 5. Plot of N/N_0 versus t/τ_{ABC} where N is the number of particles in a region of high strain rate or high vorticity and N_0 is the initial number of particles in that region. Solid lines correspond to $A=B=120$ cm/s, dashed lines to $A=B=60$ cm/s, and dotted lines to $A=B=10$ cm/s. Solid symbols correspond to the region of large rate of strain and open symbols correspond to the region of large vorticity: Squares: $a=8.075\times10^{-5}$ cm; circles: $a=8.5\times10^{-5}$ cm; triangles: $a=8.925\times10^{-5}$ cm. Calculation performed with $T=2$ K and $\rho_p=1.1$ g/cm^3.

the flow. The first is the region where the vorticity $\boldsymbol{\omega}^{\mathrm{ABC}}$ has magnitude $\omega^{\mathrm{ABC}}=|\boldsymbol{\omega}^{\mathrm{ABC}}|$ larger than three-quarters of the maximum value, $\omega^{\mathrm{ABC}}>0.75\omega^{\mathrm{ABC}}_{\mathrm{max}}$. The second region is where the invariant e^{ABC} of the rate-of-strain tensor e^{ABC}_{ij}, given by $e^{\mathrm{ABC}}=\Sigma^3_{i=1}\Sigma^3_{j=1}e^{\mathrm{ABC}}_{ij}e^{\mathrm{ABC}}_{ij}$, exceeds three-quarters of the maximum value, $e^{\mathrm{ABC}}>0.75e^{\mathrm{ABC}}_{\mathrm{max}}$, where $e^{\mathrm{ABC}}_{i,j}$ is

$$e^{\mathrm{ABC}}_{ij}=\frac{1}{2}\left(\frac{\partial v^{\mathrm{ABC}}_i}{\partial x_j}+\frac{\partial v^{\mathrm{ABC}}_j}{\partial x_i}\right). \tag{31}$$

Figure 5 shows how the number N of particles in the two regions depends on time (scaled in units of τ_{ABC}) for numerical simulations performed using different particle sizes and ABC flow intensities (the temperature and the particle density is the same as in the previous calculation). The number N of particles in the two regions is scaled in units of N_0, which is the number of particles in each region at $t=0$ (the initial number of particles in the region of large vorticity and in the region of large strain rate are not exactly the same, due to the arbitrary definition of these regions and the randomness of the initial position of the particles). It is apparent that, as time progresses, the number of particles in the region of large rate of strain increases whereas the number of particles in the region of large vorticity decreases. The rate at which this separation occurs depends upon the size of the particles and the intensity of the flow: the stronger the eddy and the larger the particle, the more pronounced is the separation.

The use of buoyant particles reduces the segregation effect, although it does not eliminate it. We have performed calculations for buoyant particles at $T=2$ K for the same range of flow velocities and radius values centered around $a=2.525\times10^{-4}$ cm. Figure 6 shows the difference between the ensemble-averaged velocity of the particles and the ensemble-averaged velocity of the fluid at the position of the

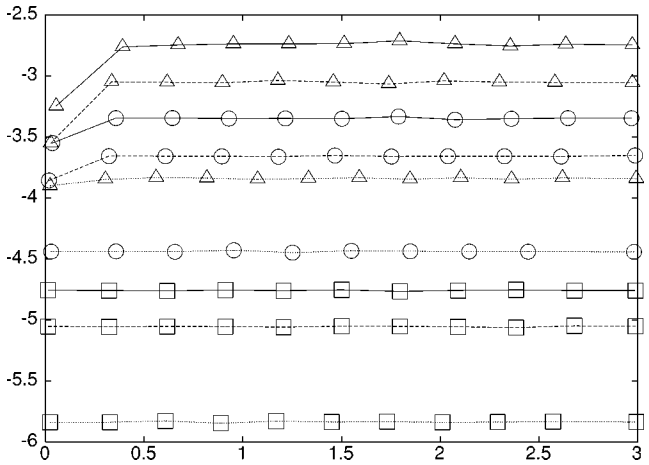

FIG. 6. Plot of $\log_{10}(\langle|\mathbf{u}_p-\mathbf{v}^{\mathrm{ABC}}|/|\mathbf{v}^{\mathrm{ABC}}|\rangle)$ as a function of t/τ_{ABC} for neutrally buoyant particles at $T=2$ K. Solid lines correspond to $A=B=120$ cm/s, dashed lines to $A=B=60$ cm/s, and dotted lines $A=B=10$ cm/s. The symbols correspond to different values of the radius of the particles: Squares: $a=5.0\times10^{-5}$ cm; circles: $a=2.525\times10^{-4}$ cm; triangles: $a=5.0\times10^{-4}$ cm.

particles (note the logarithmic scale): we conclude that the particles trace the fluid well. We find that the quantities $\langle|\mathbf{u}_p|\rangle$ and $\langle|\mathbf{v}^{\mathrm{ABC}}|\rangle$ do not change with time during the time scale under consideration (up to three times the value of τ/τ_{ABC}), which suggests that there is no segregation. To confirm this result we have plotted the position of the particles in the (x,z) plane, and found that the initial random scatter is preserved. Indeed, Fig. 7 shows that the normalized numbers of particles in the region of large strain rate and in the region of large vorticity do not change as the time progresses (compare the vertical scale against the vertical scale of Fig. 5). It

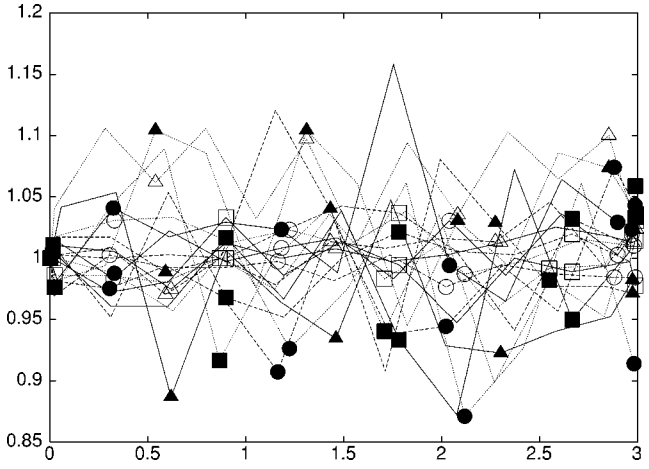

FIG. 7. Plot of N/N_0 versus t/τ_{ABC} where N is the number of particles in the region of large strain rate and in the region of large vorticity, and N_0 is the initial number of particles in that region. Solid lines correspond to $A=B=120$ cm/s, dashed lines to $A=B=60$ cm/s, and dotted lines to $A=B=10$ cm/s. Solid symbols refer to large rate of strain and open symbols refer to large vorticity. Squares: $a=5.0\times10^{-5}$ cm; circles: $a=2.525\times10^{-4}$ cm; triangles: $a=5.0\times10^{-4}$ cm. Calculation performed with buoyant particles for $T=2$ K.

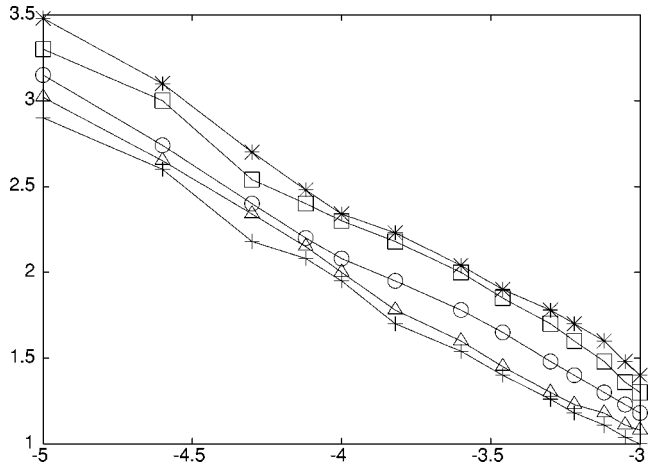

FIG. 8. $(\log_{10}A,\log_{10}\tau)$ plane. The domain above the curve identified by the value of parameter γ corresponds to the segregation of particles within three turnover times of the ABC flow. Crosses: $\gamma=0.05$; triangles: $\gamma=0.1$; circles: $\gamma=0.5$; squares: $\gamma=1.0$; stars: $\gamma=1.2$.

would be wrong however to conclude that buoyant particles are immune from segregation: the instability simply requires a longer time scale to be visible (about ten times τ/τ_{ABC} with the parameters used). Since this time scale is significantly larger than the lifetime of the eddies in real turbulence (the turnover time), segregation has no effect on PIV. We note that this absence of effective segregation is an added reason for choosing to use neutrally buoyant particles.

To quantify the segregation in the ABC flow, we introduce the quantity N^s/N_0^s where N^s is the number of particles in a region of high rate of strain and N_0^s is the initial number of particles in that region. Based on a visual perception of the results illustrated by Figs. 4 and 5, we suggest the following criterion for particle segregation in the ABC flow. We say that the particles have segregated if, after three turnover times of the ABC flow, the quantity N^s/N_0^s becomes greater than 2. Since the particle motion in the ABC flow is determined by the parameters τ and γ [see Eq. (29)] and the flow strength A, the proposed criterion enables us to identify in (τ,γ,A) space the domain corresponding to the particle segregation within three turnover times. In (A,τ) plane such a domain is located above the curve defined by the value of the parameter γ; see Fig. 8.

VIII. TRAPPING OF PARTICLES ON VORTEX LINES

We have repeatedly stressed that our discussion so far has been based on the assumption that the tracer particles do not become trapped on vortex lines in the superfluid component. We must now discuss whether this assumption is justified. We shall find that in many cases of practical interest it is not justified, and in these cases we must discuss the resulting effect on the motion of the particles. For the sake of simplicity, we shall only consider the interaction of a single particle with a single vortex; in reality, it is possible that many vortices become trapped onto the same particle, as in some experiments the estimated intervortex spacing is of the order of the particle size.

We note first that when a particle of radius a is trapped on a vortex the energy of the helium is reduced by an amount approximately equal to the kinetic energy of the displaced superfluid. It is easy to see that this kinetic energy is given approximately by

$$E_s = \frac{\rho_s \kappa^2 a}{4\pi} \log(a/\xi_0), \tag{32}$$

where $\kappa = h/m_4 \approx 10^{-3}$ cm^2 s^{-1} is the quantum of circulation in He II. For typical particle sizes $E_s \gg k_B T$, where k_B is Boltzmann's constant, so that thermal effects do not inhibit trapping.

We confine our attention to neutrally buoyant particles. Let us first consider an initial condition in which a particle is at rest at a distance r_0 from an isolated stationary rectilinear vortex, the normal fluid being also at rest. We assume for the present that the vortex line does not move in response to any movement of the particle. Then, from Eq. (10), for the case of a neutrally buoyant particle ($\rho_0 = 3\rho/2$) the equation of motion of the particle is

$$\frac{d\mathbf{u}_p}{dt} = -\frac{1}{\tau}\mathbf{u}_p + \frac{3\rho_s}{2\rho_o}(\mathbf{v}_s \cdot \boldsymbol{\nabla})\mathbf{v}_s, \tag{33}$$

where $\mathbf{v}_s$ remains equal to that due to a stationary vortex; i.e., $\mathbf{v}_s = [0, \kappa/(2\pi r), 0]$ (cylindrical polar coordinates).

If the viscous term, $-\mathbf{u}_p/\tau$, vanishes, then Eq. (33) has a solution corresponding to the particle moving in a circular orbit round the vortex with velocity $\mathbf{j}/\rho = (\rho_s/\rho)\mathbf{v}_s$.

For neutrally buoyant particles of the size $a = 1$ μm, the particle relaxation time is $\tau = \rho a^2/(3\mu_n) \sim 2 \times 10^{-5}$ s. This time is much smaller than the time taken for the particle to orbit around the vortex if r_0 is comparable with typically relevant values, which must be of the order of the vortex spacing ℓ in a turbulent superfluid. Thus any orbital motion will be strongly damped, as will be any motion along the vortex.

Thus we can focus on motion of the particle in the radial direction, which is driven by the radial term $(\mathbf{v}_s \cdot \boldsymbol{\nabla})\mathbf{v}_s$, and which has the form of a radial pressure-gradient force $\boldsymbol{\nabla}(1/r^2)$. Let u_p denote the radial component of $\mathbf{u}_p$. We have

$$\frac{du_p}{dt} = -\frac{u_p}{\tau} - \frac{2\beta}{r^3}, \tag{34}$$

where $\beta = \rho_s \kappa^2/(8\pi^2\rho) \sim 0.79 \times 10^{-8}$ cm^4 s^{-2} (here and below in this section the numerical values of parameters are calculated at the temperature 1.85 K).

It can be expected that the particle acceleration is small (we will justify this assumption later), so that the particle motion is governed by the balance of the friction and the pressure gradient force, i.e., $\tau^{-1}u_p + 2\beta r^{-3} = 0$. But $u_p = dr/dt$ so this equation takes the form

$$r^3 dr/dt = -2\beta\tau. \tag{35}$$

The solution is

$$r^4 = -8\beta\pi t + r_0^4. \tag{36}$$

Estimating now $du_p/dt = d^2r/dt^2$ from the solution (36) we find

$$du_p/dt = -12(\beta\tau)^2(-8\beta\pi t + r_0^4)^{-7/4} \tag{37}$$

and, clearly, since $\beta\tau \approx 2.8 \times 10^{-13}$ s^{-1} (for the case of 1 μm particles), the acceleration can be neglected until the moment when the particle reaches the close vicinity of the vortex core. This is consistent with the approximation in Eq. (35).

It is convenient to divide the radial motion of the particle into two stages. In the first stage the particle, which starts at $t = 0$ at distance r_0 from the vortex, approaches the vortex up to some distance of the order, say, of $2a$, without disturbing the vortex significantly. The time t_a required for the particle to travel from $r = r_0$ to $r = 2a$ is given by $(2a)^4 = -8\beta\pi t_a + r_0^4$, which is

$$t_a = \frac{r_0^4}{8\beta\tau}\left(1 - \frac{(2a)^4}{r_0^4}\right). \tag{38}$$

In the second stage our assumption that the position of vortex remains unperturbed by the approaching particle must fail; the vortex must become curved, effectively due to the presence of an image vortex in the particle, and it must move. Eventually it connects to the particle; at this point the vortex length and thus the kinetic energy of the superfluid around the vortex, rapidly decrease, until what is left at the final time t_0 is the particle trapped on the vortex. Clearly this presumed scenario is only an educated guess; the details of the relative motion of vortex and particle may be rather complicated, particularly during the second stage: the motion becomes of a three-dimensional nature, and it may involve the generation of Kelvin waves on the vortex, which may add to the loss of energy due to viscous dissipation. We do not know how long the second stage takes, but we guess that it is less than t_a. Thus t_a is our estimate for the trapping time of a particle released from rest at a distance r_0 from an isolated rectilinear vortex.

We must now consider how this result relates to trapping in a random tangle of vortex lines, such as will often exist approximately on a length scale comparable with the line spacing ℓ. These lines will be in continual motion with velocities of the order $v_L = \kappa/(2\pi\ell)$. There may be an additional velocity, due to local overall motion of the lines, but v_L is likely to represent a minimum value. The normal fluid velocity is likely to be largely uncorrelated to v_L on the scale ℓ, so the velocity of the normal fluid relative to the superfluid vortex lines is likely to be fluctuating and not less than v_L.

If the relaxation time (11) (for a neutrally buoyant particle) is small, the particles will move generally with the normal fluid, so that they will move with the velocity v_L relative to the superfluid vortex lines. The fact that the motion of the vortex lines is not regular does not affect the validity of the following argument.

We introduce a capture cross section, b_c, to describe the probability of capture of a particle by a vortex line within the tangle. The mean free path for capture is then given by $L_p = \ell^2/b_c$, and the mean free time by $T_p = \ell^2/(b_c v_L)$. The cross section b_c can presumably be obtained from computer simulations, although the need to take account of the movement

of the vortex line in response to the presence of the particle makes it nontrivial. We can, however, make a preliminary estimate as follows. As already shown, the capture time from a distance r_0 for a particle initially at rest is given roughly by $t_a \approx r_0^4/(8\beta\tau)$ [Eq. (38)]; i.e., by

$$t_a = \frac{\pi^2 \rho r_0^4}{\rho_s \kappa^2 \tau} = \frac{3\pi^2 \mu_n r_0^4}{\rho_s \kappa^2 a^2}. \tag{39}$$

Now suppose that a particle, moving with velocity v_L, approaches the vortex line with an impact parameter r_0. It will probably be captured if the time it spends at a distance of about r_0 from the line is greater than t_a, i.e., if

$$\frac{r_0}{v_L} > \frac{3\pi^2 \mu_n r_0^4}{\rho_s \kappa^2 a^2}. \tag{40}$$

It follows that our estimated capture cross section is given by

$$b_c^3 = \frac{\rho_s \kappa^2 a^2}{3\pi^2 \mu_n v_L} = \frac{2\rho_s \kappa a^2 \ell}{3\pi\mu_n}, \tag{41}$$

and the mean free time by

$$T_p = 1.68 \frac{2\pi\ell^2}{\kappa} \left(\frac{\mu_n}{\rho_s \kappa} \frac{\ell^2}{a^2} \right)^{1/3}. \tag{42}$$

The ratio $\mu_n/(\rho_s\kappa)$ is typically about 0.1, and therefore

$$T_p \sim \frac{2\pi\ell^2}{\kappa} \left(\frac{\ell}{a} \right)^{2/3}. \tag{43}$$

The quantity $2\pi\ell^2/\kappa$ is the time $\tau(\ell)$ that characterizes the evolution of the turbulence on the scale ℓ; it is the effective turnover time on scale ℓ. We have already noted that a ought to be less than the minimum length scale in the turbulence, and therefore that a ought to be less than ℓ. Thus mean free time will be larger than $\tau(\ell)$. In experiments[5] ℓ varies from 3 μm to 100 μm. In practice a cannot be much less than 1 μm, so that the mean free time varies from about 1 ms to about 10 s. Observations in which particle trapping does not occur might be possible at the upper end of this range of mean free times, but not at the lower end. It must be noted, however, that if there were a large average value of $|\mathbf{v}_n - \mathbf{v}_s|$, the capture time T_p would be less than that indicated by Eq. (43), and observations in which trapping does not occur would become more difficult.

It might be thought at first sight that, if trapping does occur, the particles will move on average with the velocity of the unperturbed vortex lines. Unfortunately, this is not generally true, for two reasons. First, the presence of a particle at a particular point on a vortex line can modify the motion of the line [the motion of free line relative to the local superfluid velocity is determined by the Magnus effect, $\mathbf{f} = \rho_s \kappa \times (\mathbf{v}_L - \mathbf{v}_s)$, where $\mathbf{f}$ is the force of mutual friction between the line and the normal fluid; this force is effectively modified locally if a particle is attached to the line]. Secondly, if the normal fluid is flowing locally with a velocity that has a component parallel to the vortex line, then the viscous force on the particle will cause it to move along the line. These effects are clearly rather complicated, and their elucidation will require further work.

We consider three particular cases of special interest, and discuss the importance of trapping in each case.

The first is *vortex-coupled turbulence*, already discussed in earlier sections. In this case, as we have already noted, the two fluids have the same velocity fields on scales greater than ℓ, and the vortices can be expected to move on these large scales with this same common velocity. Whether trapping occurs is then unimportant. On scales comparable with ℓ the different velocity fields do not coincide, and trapping will then have a rather complicated effect.

The second is *superfluid turbulence at a very low temperature*, where the normal fluid is effectively absent. Our calculation of the mean free time associated with trapping is then inapplicable. However, in this case the vortex lines move with the local superfluid velocity, and there is no normal fluid and no mutual friction. Therefore it is probable that whether or not trapping occurs is unimportant, and, apart from transients, the particles will follow the superfluid.

The third case is *thermal counterflow turbulence* above 1 K. This is the only case for which there exist any experimental results.[12] We have noted the argument of Sec. VI B that in the absence of trapping the particles can be expected to follow on average the motion of the normal fluid. This is not in accord with experiment. The vortex line spacings in the experiments are such that the mean free time for trapping is likely to be not more than 30 ms, so that in practice trapping is very likely to have occurred.

It is interesting to consider in connection with thermal counterflow turbulence a very simple, but, as it turns out, inadequate model for the mean particle velocities in the presence of trapping. Suppose that the vortex tangle in counterflow turbulence is isotropic and moves with the superfluid component. There is evidence, from both experiment and theory[1] that it does move with the superfluid, at least approximately, but it is not quite isotropic, the lines tending to point preferentially in directions normal to the heat flow, especially at higher temperatures. Suppose further than the trapped particles do not have a significant influence on the local motion of the lines, and that viscous interaction of a particle with the normal fluid causes the particle to move along the line at a rate given by the Stokes law with the force equal to the component of the viscous force along the line. It is then easy to show that the particles can be expected to move at an average velocity relative to the superfluid equal to one-third of the relative velocity between the two fluids, the factor of one-third arising from the average value of $\cos^2\theta$ over a sphere, where θ is a polar angle relative to the direction of heat flow. Experiment shows that the particles move with an average velocity equal to one-half of the normal fluid velocity.[12] The discrepancy is in the wrong direction to be due to lack of isotropy in the vortex tangle. However, as we have already emphasized, the trapped particles must almost certainly modify the local motion of the vortices, and this may be the reason for the discrepancy. Development of this idea poses severe problems. We emphasize that in this case the particles appear not to respond in any simple way to the flow.

IX. CONCLUSION

We have set up the governing equations of motion for particles in He II, highlighting the approximations and the

limitations of these equations. By solving some simple one-dimensional problems, we have identified various regimes, which are particularly simple if the particles are neutrally buoyant. These regimes correspond to the particles tracing the motion of the superfluid, the normal fluid or the total mass current $\mathbf{j}/\rho$. These solutions allow us to gain physical insight into the nature of the motion of particles in turbulent flows. In the case where the superfluid and normal fluid velocity fields are essentially the same on a large range of length scales, we find that, if the eddy turnover time is much less than the relaxation time of the particle, the particle will move with the mass current $\mathbf{j}/\rho$; vice versa, if the turnover time is much larger than the relaxation time, the particle will move with the normal fluid, provided the trajectory of the particle is stable. At very low temperatures the particle will follow the turbulence of the superfluid.

To study the issue of the stability of the particle trajectory we have solved numerically some two-dimensional flow problems which refer to the situation in which the superfluid and normal fluid velocity fields are essentially the same over a wide range of scales. We have found that it is important to be aware of the possibility that particles segregate spatially, moving from regions of high vorticity into regions of high rate of strain; fortunately we have concluded that, using existing particles, it is possible to avoid this segregation effect.

We show that these promising results may well be invalidated when we take into account the trapping of particles by the vortex lines, unless the density of vortex lines is very small and smaller than is often the case in practice. We show that in some simple cases, notably vortex-coupled superfluid turbulence and superfluid turbulence at a very low temperature, trapping does not invalidate some rather simple results. But in other cases, such as thermal counterflow turbulence, trapping has probably a serious effect, which is hard to interpret.

We hope that this work will encourage further experiments, including laminar regimes which are important to test our understanding of the interaction between particles and He II. On the theoretical side, the next step is clearly to move to three-dimensional simulations which can more properly include the presence of the quantized vortices, and to simulations that take proper account of trapping.

ACKNOWLEDGMENTS

The research described in this article was made possible due to the participation of C.F.B. and Y.A.S. in the Grant GR/T08876/01 of the UK Engineering and Physical Sciences Research Council. C.F.B. is grateful to Professor S. VanSciver for stimulating his interest in this investigation. Y.A.S. and C.F.B. are also grateful to Professor C. Vassilicos and Professor M. Reeks for fruitful discussions and support in initiating this new research area.

APPENDIX: FORCE ACTING ON A PARTICLE IN THE NONUNIFORM FLOW

1. Sphere in the inviscid unsteady nonuniform irrotational flow

Subsections 1 and 2 are based on the approach developed in Ref. 14.

We assume below that the body force is absent and consider a spherical particle moving with velocity $\mathbf{u}_p$ in the irrotational flow field $\mathbf{v}(\mathbf{r},t)$ of the inviscid fluid. We assume that the size of the particle is much smaller than the characteristic length scale of the flow, i.e.,

$$\varepsilon = a\|\nabla \mathbf{v}_0\|/W \ll 1, \tag{A1}$$

where $\mathbf{v}_0$ is the ambient velocity field of the fluid, $\mathbf{W}=\mathbf{V}-\mathbf{u}_p$ the relative velocity between the ambient flow at the position of the center of the sphere and the particle, $\mathbf{V}(t)=\mathbf{v}_0(\mathbf{R}(t),t)$, $\mathbf{R}(t)$ being the position of the center of the particle. Assumption (A1) means that it will be sufficient to consider only uniform-straining fields of the fluid velocity. It is also assumed that the timescale of change in $\mathbf{W}$ is large compared with the time required for a fluid to pass around the particle.

The relative velocity field around the particle, $\mathbf{w}=\mathbf{v}-\mathbf{u}_p$ is the solution of the Euler and continuity equations subject to the condition of zero flux through the particle surface; at large distances from the sphere $\mathbf{w}\to\mathbf{v}_0-\mathbf{u}_p$. In the reference frame moving with the particle, $\mathbf{r}'=(x_1',x_2',x_3')$, the relative flow field, $\mathbf{w}(\mathbf{r}',t)$ can be represented as the sum of the uniform "far-field" flow $\mathbf{W}$, the perturbation $\Delta\mathbf{w}^{(\mathrm{U})}$ caused by the sphere, and the extensional flow $\Delta\mathbf{w}^{(\mathrm{E})}$, i.e.,

$$\mathbf{w} = \mathbf{W} + \Delta\mathbf{w}^{(\mathrm{U})} + \Delta\mathbf{w}^{(\mathrm{E})}. \tag{A2}$$

The perturbation $\Delta\mathbf{w}^{(\mathrm{U})}$ is of the same order of magnitude as $\mathbf{W}$, while $|\Delta\mathbf{w}^{(\mathrm{E})}|/W=O(\varepsilon)$. Since the flow field $\mathbf{w}$ is irrotational, $\mathbf{w}=\nabla\phi$ where

$$\phi = \phi_0 + \phi^{(\mathrm{U})} + \phi^{(\mathrm{E})}. \tag{A3}$$

The potential of the uniform flow is $\phi_0=\mathbf{W}\cdot\mathbf{r}'$. The potential of the zero-order perturbation of the uniform flow $\Delta\mathbf{w}^{(\mathrm{U})}$ caused by the sphere is $\phi^{(\mathrm{U})}=C^{(\mathrm{U})}(r')\mathbf{W}\cdot\mathbf{r}'$, where $r'=|\mathbf{r}'|$, and, for a spherical particle, $C^{(\mathrm{U})}(r')=a^3/(2r'^3)$. Finally, for the potential of the extensional flow we have $\phi^{(\mathrm{E})}=e_{ij}x_i'x_j'$, where $e_{ij}=$const are the components of the rate-of-strain tensor.

To calculate the force acting on the particle, the Euler equation must be formulated in the noninertial reference frame moving with the particle:

$$\frac{\partial\mathbf{w}}{\partial t} + (\mathbf{w}\cdot\nabla)\mathbf{w} = -\frac{1}{\rho}\nabla p' - \frac{d\mathbf{u}_p}{dt}, \tag{A4}$$

where the last term represents the D'Alembert force, and p' is the fluid pressure in the noninertial reference frame. The force acting on the particle is

$$\mathbf{F} = -\int_S p'\mathbf{n}\,dS, \tag{A5}$$

where S is the surface of the particle. Since the flow is irrotational, we have $(\mathbf{w}\cdot\nabla)\mathbf{w}=\frac{1}{2}\nabla(\mathbf{w}\cdot\mathbf{w})$. Now, using the Cauchy-Lagrange integral, written in the noninertial reference frame as

$$\rho\left(\frac{\partial\phi}{\partial t}+\frac{1}{2}\mathbf{w}\cdot\mathbf{w}+\frac{d\mathbf{u}_p}{dt}\cdot\mathbf{x}'\right)+p'=f(t), \tag{A6}$$

where $f(t)$ is the function which can be determined from the conditions at $|\mathbf{x}'|\to\infty$, and making use of the gradient theorem, the force acting on the particle can be calculated as

$$\mathbf{F}=\rho\int_S\left(\frac{\partial\phi}{\partial t}+\frac{1}{2}\mathbf{w}\cdot\mathbf{w}\right)\mathbf{n}dS+\rho\vartheta\frac{d\mathbf{u}_p}{dt}. \tag{A7}$$

Taking into account that the term $(\mathbf{W}+\boldsymbol{\nabla}\phi^{(\mathrm{U})})\cdot(\mathbf{W}+\boldsymbol{\nabla}\phi^{(\mathrm{U})})$ is symmetric with respect to the center of the sphere [and, therefore, its contribution to integral (A7) is zero], and making use of the perturbation technique for expansion (A2) (in terms of ε), the force acting on the sphere can be represented as

$$\frac{\mathbf{F}}{\rho}=\int_S\left(\frac{\partial\phi_0}{\partial t}+\frac{\partial\phi^{(\mathrm{U})}}{\partial t}\right)\mathbf{n}dS+\int_S(\mathbf{W}+\boldsymbol{\nabla}\phi^{(\mathrm{U})})\cdot\boldsymbol{\nabla}\phi^{(\mathrm{E})}\mathbf{n}dS+\vartheta\frac{d\mathbf{u}_p}{dt}. \tag{A8}$$

Incorporating the potentials ϕ_0, $\phi^{(\mathrm{U})}$ and $\phi^{(\mathrm{E})}$ and making use again of the gradient theorem, one finds

$$F_i=\rho\vartheta\{(1+C)(\dot{W}_i+e_{ij}W_j)+(\dot{u}_p)_i\}, \tag{A9}$$

where $C=C^{(\mathrm{U})}(r')|_{r'=a}=1/2$ is the added mass coefficient, and $\dot{(\cdot)}\equiv d/dt$. Since $\mathbf{W}=\mathbf{V}-\mathbf{u}_p$, we write

$$\dot{W}_i+e_{ij}W_j=\frac{\partial v_{0i}}{\partial t}+e_{ij}v_{0j}-(\dot{u}_p)_i, \tag{A10}$$

where the right-hand side is evaluated at the position of the particle center. Because $e_{ij}v_{0j}\equiv v_{0j}\partial v_{0i}/\partial x_j'$, we have

$$\dot{W}_i+e_{ij}W_j\equiv\frac{Dv_{0i}}{Dt}-\frac{d(u_p)_i}{dt}, \tag{A11}$$

so that the fluid-particle interaction force takes the form

$$\mathbf{F}=\rho\vartheta\frac{D\mathbf{v}}{Dt}+C\rho\vartheta\left(\frac{D\mathbf{v}}{Dt}-\frac{d\mathbf{u}_p}{dt}\right), \tag{A12}$$

where the subscript "0" is now omitted, and $\mathbf{v}$ should be understood as the ambient flow field of the fluid.

2. Sphere in the inviscid unsteady nonuniform rotational flow

We assume now that the vorticity of the ambient flow $\boldsymbol{\omega}_0=\boldsymbol{\nabla}\times\mathbf{v}_0$ is not zero, but all other assumptions formulated in the previous subsection remain valid. In the uniform straining flow the vorticity is also uniform. Since $|\boldsymbol{\omega}|\approx\|\boldsymbol{\nabla}\mathbf{v}_0\|$, the rate of change of vorticity can be estimated as $|\partial\boldsymbol{\omega}/\partial t|\approx|(\boldsymbol{\omega}\cdot\boldsymbol{\nabla})\mathbf{v}_0|\approx\|\boldsymbol{\nabla}\mathbf{v}_0\|^2$, so that on the time scale characteristic of the flow past a sphere the relative change in the far-field vorticity is $|\delta\boldsymbol{\omega}|\approx a\|\boldsymbol{\nabla}\mathbf{v}_0\|/W\ll|\boldsymbol{\omega}|$. In terms of small parameter ε the above means that, to $O(\varepsilon)$, $\partial\boldsymbol{\omega}/\partial t=0$, so that the relative flow field can be represented by the asymptotic expansion [similar to Eq. (A2)]

$$\mathbf{w}=\mathbf{W}+\Delta\mathbf{w}^{(\mathrm{U})}+\Delta\mathbf{w}^{(\mathrm{E})}+\Delta\mathbf{w}^{(\omega)}, \tag{A13}$$

where the first three terms are the same as in Eq. (A2), and the order of magnitude of the rotational contribution $\Delta\mathbf{w}^{(\omega)}$ is $|\Delta\mathbf{w}^{(\omega)}|/W=O(\varepsilon)$. Based on the asymptotic expansion in terms of ε, the calculation of the force $\mathbf{F}$ is similar to that of the previous subsection (for details see Ref. 14). The fluid-particle interaction force can be represented as the sum of the force (A12) and the rotational contribution, i.e.,

$$\mathbf{F}=\rho\vartheta\frac{D\mathbf{v}}{Dt}+C\rho\vartheta\left(\frac{D\mathbf{v}}{Dt}-\frac{d\mathbf{u}_p}{dt}\right)+\mathbf{F}^{(\omega)}, \tag{A14}$$

where

$$\mathbf{F}^{(\omega)}=\rho\vartheta C_{\mathrm{L}}(\mathbf{v}-\mathbf{u}_p)\times\boldsymbol{\omega} \tag{A15}$$

[in Eqs. (A14) and (A15) the subscript "0" is omitted, so that $\mathbf{v}$ and $\boldsymbol{\omega}$ refer to the ambient flow field]. Physically, the contribution $\mathbf{F}^{(\omega)}$ arises due to stretching of vortex lines. In Eq. (A15) C_{L} is the lift coefficient; for a sphere $C_{\mathrm{L}}=1/2$. The right-hand sides of Eqs. (A14) and (A15) are evaluated at the center of the sphere.

3. Spherical particle in the unsteady nonuniform viscous flow

Here the situation is more complicated because the analysis of the unsteady particle motion in an arbitrary nonuniform flow is no longer possible. Maxey and Riley[15] studied analytically the unsteady motion of a sphere in an arbitrary creeping flow and obtained the following result for the fluid-particle interaction force:

$$\mathbf{F}=\mathbf{F}^{(\mathrm{d})}+C\rho\vartheta\left(\frac{d\mathbf{v}}{dt}-\frac{d\mathbf{u}_p}{dt}\right)+\rho\vartheta\frac{D\mathbf{v}}{Dt}+\mathbf{F}_{\mathrm{B}}, \tag{A16}$$

where the first term $\mathbf{F}^{(\mathrm{d})}=6\pi a\rho\nu(\mathbf{v}-\mathbf{u}_p)$ represents the viscous drag in the case where the particle Reynolds number $\mathrm{Re}_p\ll1$, and $\mathbf{F}^{(\mathrm{B})}$ is the Basset (history) force. It is important to emphasize that the analysis[15] was performed for a creeping flow where the derivative of the fluid velocity $d\mathbf{v}/dt$, seen by the particle, and the substantial derivative $D\mathbf{v}/Dt$ cannot be distinguished. In Ref. 15 it was found that the added mass coefficient C for a spherical particle in a viscous flow is precisely the same as for a sphere in an inviscid fluid, $C=1/2$.

Based on the observation that, in the case of unsteady, spatially uniform flow, the form and the physical interpretation of the second and the third terms in Eq. (A16) coincide with the form and interpretation of the similar terms in the force (A12), Mei[16] proposed that, for an arbitrary nonuniform viscous flow, the force (A16) should be generalized as follows:

$$\mathbf{F}=6\pi a\rho\nu(\mathbf{v}-\mathbf{u}_p)+C\rho\vartheta\left(\frac{D\mathbf{v}}{Dt}-\frac{d\mathbf{u}_p}{dt}\right)+\rho\vartheta\frac{D\mathbf{v}}{Dt}+\mathbf{F}_{\mathrm{B}}. \tag{A17}$$

The numerical study[18] of the accelerated sphere's motion in the steady straining flow confirmed that the value of the

added mass coefficient, $C=1/2$ remains valid for higher particle Reynolds numbers and strongly nonuniform flows. In general, the added mass coefficient depends only on the particle geometry.

The Basset force has the form

$$\mathbf{F}_{\mathrm{B}} = 6\pi a\rho\nu \int_{-\infty}^{t} K(t-\tau,\tau)\frac{d(\mathbf{v}-\mathbf{u}_p)}{d\tau}d\tau. \qquad \text{(A18)}$$

The comprehensive study of the kernel $K(t-\tau,\tau)$ can be found in Ref. 17. We only note that for relatively short time

$$K(t-\tau,\tau) = \frac{a}{\sqrt{\pi\nu(t-\tau)}}, \qquad \text{(A19)}$$

but the behavior of the integral kernel becomes more complicated for larger times; in particular, as $t\to\infty$ the history kernel decays much faster than $t^{-1/2}$.

Further generalizations include a modification (by numerous authors; see, e.g., Ref. 33 and references therein) of the viscous drag term for the case of higher particle Reynolds numbers, e.g.,

$$\mathbf{F}^{(\mathrm{d})} = \frac{1}{2}C_D(\mathrm{Re}_p)\pi a^2\rho|\mathbf{v}-\mathbf{u}_p|(\mathbf{v}-\mathbf{u}_p), \qquad \text{(A20)}$$

and also modifications of the kernel (A19) for the case of high initial relative velocity between the fluid and the particle.

The force in the form (A17) was derived in the case of weak shear. In the case where shear is sufficiently strong, the Saffman lift force $\mathbf{F}^{(\omega)}$ should also be included in Eq. (A17); see, e.g., Refs. 34 and 35. In the case of simple shear such that $v_x=v_x(y)$, $v_y=v_z=0$ the lift force is

$$F_y^{(\omega)} = 6.46\rho\nu^{1/2}a^2\sqrt{\frac{dv_x}{dy}}[v_x-(u_p)_x], \quad F_x^{(\omega)}=F_z^{(\omega)}=0. \qquad \text{(A21)}$$

In the case where the finite relative velocity $\mathbf{u}_p-\mathbf{v}$ between the particle and the fluid is combined with rotation of the particle, a transverse force known as the Magnus lift force should be included in Eq. (A17) as well. This force arises due to asymmetry of streamlines in the vicinity of the rotating sphere. In the case where the particle Reynolds number Re_p and the rotational Reynolds number $\mathrm{Re}_\Omega = 4\rho|\mathbf{\Omega}|a^2/\mu$, where $\mathbf{\Omega}$ is the angular velocity of the particle rotation, are small, this force was calculated in Ref. 23 in the form

$$\mathbf{F}^{(\mathrm{LM})} = \pi a^3\rho\mathbf{\Omega}\times(\mathbf{u}_p-\mathbf{v}). \qquad \text{(A22)}$$

[1] R. J. Donnelly, *Quantised Vortices In Helium II* (Cambridge University Press, Cambridge, England, 1991).
[2] R. J. Donnelly and C. F. Barenghi, J. Phys. Chem. Ref. Data **27**, 1217 (1988).
[3] C. F. Barenghi, R. J. Donnelly, and W. F. Vinen, *Quantized Vortex Dynamics And Superfluid Turbulence*, (Springer, Berlin, 2001).
[4] M. R. Smith, R. J. Donnelly, N. Goldenfeld, and W. F. Vinen, Phys. Rev. Lett. **71**, 2583 (1993).
[5] S. R. Stalp, L. Skrbek, and R. J. Donnelly, Phys. Rev. Lett. **82**, 4831 (1999).
[6] J. Maurer and P. Tabeling, Europhys. Lett. **43**, 29 (1998).
[7] W. F. Vinen and J. J. Niemela, J. Low Temp. Phys. **129**, 213 (2002).
[8] C. F. Barenghi, S. Hulton, and D. C. Samuels, Phys. Rev. Lett. **89**, 275301 (2002).
[9] R. G. Matley, W. Y. T. Wong, M. S. Thurlow, P. G. J. Lucas, M. J. Lees, O. J. Griffiths, and A. L. Woodcraft, Phys. Rev. E **63**, 045301 (2001).
[10] R. J. Donnelly, A. N. Karpetis, J. J. Niemela, K. R. Sreenivasan, W. F. Vinen, and C. M. White, J. Low Temp. Phys. **126**, 327 (2002).
[11] D. Celik and S. W. VanSciver, Exp. Therm. Fluid Sci. **26**, 971 (2002).
[12] T. Zhang and S. W. Van Sciver, in *Advances in Cryogenics Engineering*, edited by S. Breon *et al.*, AIP Conf. Proc. No. 613 (AIP, Melville, NY, 2002), p. 1372.
[13] T. Zhang, D. Celink, and S. W. Van Sciver, J. Low Temp. Phys. **134**, 985 (2004).
[14] T. R. Auton, J. C. R. Hunt, and M. Prud'homme, J. Fluid Mech. **197**, 241 (1988).
[15] M. R. Maxey and J. J. Riley, Phys. Fluids **26**, 883 (1983).
[16] R. Mei, J. Fluid Mech. **270**, 133 (1994).
[17] I. Kim, S. Elghobashi, and W. A. Sirignano, J. Fluid Mech. **367**, 221 (1998).
[18] J. Magnaudet, M. Rivero, and J. Fabre, J. Fluid Mech. **284**, 97 (1995).
[19] G. I. Taylor, Proc. R. Soc. London, Ser. A **120**, 260 (1928).
[20] J. C. H. Fung, J. R. C. Hunt, and R. J. Perkins, Proc. R. Soc. London, Ser. A **459**, 445 (2003).
[21] J. C. H. Fung and J. C. Vassilicos, Phys. Rev. E **68**, 046309 (2003).
[22] I. Eames and M. A. Gilbertson, J. Fluid Mech. **498**, 183 (2004).
[23] S. I. Rubinow and J. B. Keller, J. Fluid Mech. **11**, 447 (1961).
[24] A. M. Ahmed and S. Elghobashi, Phys. Fluids **13**, 3346 (2001).
[25] J. Magnaudet and I. Eames, Annu. Rev. Fluid Mech. **32**, 659 (2000).
[26] A. Babiano, J. H. E. Cartwright, O. Piro, and A. Provenzale, Phys. Rev. Lett. **84**, 5764 (2000).
[27] T. Dombre, U. Frisch, J. M. Greene, M. Hendon, A. Mehr, and A. M. Soward, J. Fluid Mech. **167**, 353 (1986).
[28] A. D. Gilbert and S. Childress, *Stretch, Twist, Fold, the Fast Dynamo* (Springer, Berlin, 1995).
[29] A. D. Gilbert, N. F. Otani, and S. Childress, in *Solar and Planetary Dynamos*, edited by M. R. E. Proctor, P. C. Matthews and A. M. Rucklidge (Cambridge University Press, Cambridge, England, 1993), pp. 129–136.
[30] D. J. Galloway and M. R. E. Proctor, Nature (London) **356**, 691 (1992).

[31] C. F. Barenghi, D. C. Samuels, G. H. Bauer, and R. J. Donnelly, Phys. Fluids **9**, 2631 (1997).

[32] For example, an equation of the form $du/dt=f(u,t)$ is time stepped using the recursion formula

$$u_{n+1}^{k+1} = u_n^k + \frac{\Delta t}{2}[f(u_{n+1}^k) + f(u_n)],$$

where u_n^k is the kth approximation to $u(t_n)$, $t_n=n\Delta t$ ($n=1,2,\ldots$) and the time step Δt is at least 100 times smaller than the turnover time τ_{ABC}. The inner iterations $k=1,2,\ldots$ are performed until $|u_{n+1}^{k+1}-u_{n+1}^k|$ is smaller than an assigned tolerance.

[33] A. Berlemont, P. Desjonqueres, and G. Gouebet, Int. J. Multiphase Flow **16**, 19 (1990).

[34] P. G. Saffman, J. Fluid Mech. **22**, 385 (1965).

[35] P. G. Saffman, J. Fluid Mech. **31**, 624 (1968).